



Published in final edited form as:

*J Agric Food Chem.* 2020 April 01; 68(13): 3995–4004. doi:10.1021/acs.jafc.9b07965.

## Oxidative stress induction is a rational strategy to enhance the productivity of *Antrodia cinnamomea* fermentations for the antioxidant secondary metabolite antrodin C

Peng-Fei Hu<sup>1,2</sup>, Jing Huang<sup>2</sup>, Lei Chen<sup>2</sup>, Zhongyang Ding<sup>2</sup>, Liming Liu<sup>3</sup>, István Molnár<sup>\*,4</sup>, Bo-Bo Zhang<sup>\*,1,2</sup>

<sup>1</sup>Department of Biology, College of Science, Shantou University, Shantou 515063, Guangdong, P.R. China

<sup>2</sup>Key Laboratory of Carbohydrate Chemistry and Biotechnology, School of Biotechnology, Jiangnan University, Wuxi 214122, Jiangsu, P.R. China

<sup>3</sup>State Key Laboratory of Food Science and Technology, Jiangnan University, Wuxi 214122, Jiangsu, P.R. China

<sup>4</sup>Southwest Center for Natural Products Research, The University of Arizona, 250 E. Valencia Rd., Tucson, AZ 85706, USA

### Abstract

Antioxidant metabolites contribute to alleviating oxidative stress caused by reactive oxygen species (ROS) in microorganisms. We utilized oxidative stressors such as hydrogen peroxide supplementation to increase the yield of the bioactive secondary metabolite antioxidant antrodin C in submerged fermentations of the medicinal mushroom *Antrodia cinnamomea*. Changes in the superoxide dismutase and catalase activities of the cells indicate that ROS are critical to promote antrodin C biosynthesis, while the ROS production inhibitor diphenyleneiodonium cancels the productivity-enhancing effects of H<sub>2</sub>O<sub>2</sub>. Transcriptomic analysis suggests that key enzymes in the mitochondrial electron transport chain are repressed during oxidative stress, leading to ROS accumulation and triggering the biosynthesis of antioxidants such as antrodin C. Accordingly, rotenone, an inhibitor of the electron transport chain complex I, mimics the antrodin C productivity-enhancing effects of H<sub>2</sub>O<sub>2</sub>. Delineating the steps connecting oxidative stress with increased antrodin C biosynthesis will facilitate the fine-tuning of strategies for rational fermentation process improvement.

### Graphical Abstract

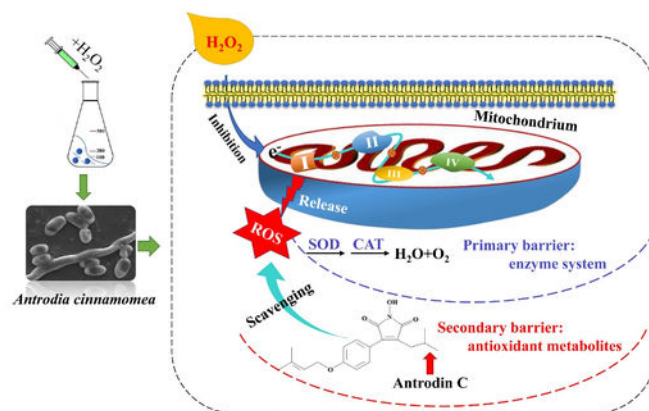
---

\*Corresponding author: István Molnár and Bo-Bo Zhang, imolnar@email.arizona.edu, superzbobo@gmail.com; Tel: +86 510 8591 8202; fax: +86 510 8591 8202.

Conflicts of interest

I.M. has disclosed financial interests in Teva Pharmaceuticals Works Ltd., Hungary and the University of Debrecen (Hungary) which are unrelated to the subject of the research presented here. All other authors declare no conflicts of interest.

E-Supplementary data of this work can be found in the online version of the paper



## Keywords

*Antrodia cinnamomea*; oxidative stress; antrodin C; submerged fermentation; transcriptomic analysis

## 1. Introduction

Medicinal fungi are unparalleled in their functional and metabolite diversity<sup>1, 2</sup>. Investigating and mimicking the natural habitats of these organisms has provided us with important clues to design new, adaptive strategies to stimulate the biosynthesis of valuable secondary metabolites (SMs) by these fungi. Thus, SM production may be elicited by environmental stimuli, such as biotic and abiotic stressors. One of the most common physiological stress conditions in the habitat of filamentous fungi is oxidative stress that leads to the formation of harmful reactive oxygen species (ROS) in the cells<sup>3,4</sup>. ROS, including hydrogen peroxide (H<sub>2</sub>O<sub>2</sub>), hydroxyl radical (HO<sup>•</sup>), and superoxide anions (O<sup>2-</sup>) cause dose-dependent damage to most biomolecules such as DNA, proteins and lipids<sup>3, 5</sup>. Microbial cells respond to ROS by initiating scavenging mechanisms, including enzymatic or non-enzymatic systems<sup>6, 7</sup>. Growing evidence also suggests that ROS play vital physiological roles in the regulation of morphogenesis, differentiation and secondary metabolism in filamentous fungi<sup>8, 9</sup>. Thus, modulation of the oxidative stress response of *Aspergillus flavus* by cinnamaldehyde effectively inhibits radial growth, spore production and mycelium formation<sup>10</sup>. Methyl jasmonate induced the biosynthesis of ganoderic acids by increasing the intracellular ROS concentration of *Ganoderma lucidum*<sup>11</sup>. Increased ROS levels were also seen to activate the transcription of a series of stress response genes such as glutathione reductase and glutathione peroxidase in *Aspergillus niger*<sup>12</sup>. Finally, stimulation of ROS production by hydrogen peroxide supplementation during the submerged fermentation of the mucoromycete *Blakeslea trispora* induced the transcription of five genes in the carotene biosynthetic pathway, leading to a substantial increase in the production of β-carotene<sup>13</sup>.

*Antrodia cinnamomea* (syn. *Taiwanofungus camphoratus*, *Antrodia camphorata* or *Ganoderma camphoratus*; Basidiomycota, Agaricomycetes, Polyporales) causes brown heart

rot disease in the small-flowered camphor tree, *Cinnamomum kanehirae*. This fungus has long been used as a traditional remedy in Taiwan against cancer, hypertension, hangover and other conditions, and preparations containing this mushroom are claimed to sell for \$100 million/year<sup>14</sup>. More than 100 bioactive compounds, including derivatives of maleic acid and succinic acid, triterpenoids, polysaccharides, ubiquinone analogues, benzenoids etc. have been isolated from fruiting bodies and mycelia of *A. cinnamomea*<sup>14–16</sup>. Among these SMs, the maleimide derivative antrodin C was shown to exhibit potent anti-inflammatory, hepatoprotective and cancer cell inhibitory activities<sup>17–20</sup>. Isolated antrodin C was shown to exert cytotoxic effects on the Lewis lung carcinoma (LLC) tumor cell line<sup>21</sup>, and to suppress epithelial to mesenchymal transition and metastasis of breast cancer cells by inhibiting the Smad2/3 and  $\beta$ -catenin signaling pathway<sup>19</sup>. Yang *et al.* showed that antrodin C promotes the interaction between autophagy and apoptosis of lung cancer cells by regulating the Akt/mTOR pathway inhibited by AMPK<sup>22</sup>. In addition, antrodin C significantly reduced the viability of lung adenocarcinoma cells (A549) *in vitro*<sup>23</sup>. These activities indicate that antrodin C is a potent lead compound for pharmaceutical drug discovery.

Interest in the continued evaluation and eventual pharmaceutical development of antrodin C as a potential human drug led to a need for rational strategies to improve the production of this compound. Thus, a novel fermentation process was established where the medium was supplemented with a surfactant and an *in situ* extractant to reduce product inhibition, leading to a sizeable increase in the yield of antrodin C fermentations (from 53 mg/L in the standard process to 247 mg/L with the modified one)<sup>24</sup>. Further analysis revealed that the *in situ* extractant not only alleviates product inhibition, but also increases dissolved oxygen concentrations during fermentation. However, this may also lead to increased intracellular ROS levels<sup>24,25</sup>. At the same time, Kumar *et al.* pointed out that antrodin C may be used to ameliorate intracellular ROS formation in human endothelial cells, suggesting that this SM may improve resistance to oxidative stress<sup>19</sup>.

In this study, we confirmed the antioxidant properties of antrodin C, and investigated the link between intracellular ROS-mediated oxidative stress and the production of antrodin C during submerged fermentations of *A. cinnamomea*. Furthermore, we used comparative transcriptomics to study the underlying mechanism by which oxidative stress regulates the biosynthesis of antrodin C. This study provides an example for a novel, rational approach that uses physiological stressors relevant to the bioactivities of the target microbial SMs to stimulate the production of these compounds.

## 2. Materials and methods

### 2.1 Strain and fermentation conditions

The strain of *A. cinnamomea* used in this study is preserved at the Key Laboratory of Industrial Biotechnology, Ministry of Education, School of Biotechnology, Jiangnan University (Wuxi, China) under accession BBZ-001. For fermentations, *A. cinnamomea* was grown on potato dextrose agar (PDA: potato 200 g/L, glucose 20 g/L, and agar 20 g/L) at 28°C for 7–14 days. The spores were collected by washing the plates with sterile distilled water and the spore suspension was adjusted to a concentration of  $1 \times 10^6$  cfu/mL. 15 mL of this suspension was used to inoculate 120 mL of seed culture medium (20 g/L glucose, 16

g/L corn steep powder, 20 mL/L soybean hydrolysate, 0.5 g/L MgSO<sub>4</sub>, 0.5 g/L K<sub>2</sub>HPO<sub>4</sub>, and 0.5 g/L citric acid; the pH was not adjusted) in a 500 mL Erlenmeyer flask, and the resulting culture was incubated for 4 days at 28°C with shaking at 130 rpm. Production cultures were inoculated with 10 mL seed culture into 500 mL Erlenmeyer flasks containing 90 mL of culture medium (40 g/L glucose, 8 g/L corn steep powder, 50 mL/L soybean hydrolysate, 0.5 g/L MgSO<sub>4</sub>, 0.5 g/L K<sub>2</sub>HPO<sub>4</sub>; the pH was not adjusted), and cultivation was continued for another 10 days at 28°C with shaking at 130 rpm.

## 2.2 Determination of biomass

Mycelia were collected from the production cultures by filtering under suction through a pre-weighted filter paper and washed with distilled water. The collected mycelia were dried at 50°C until constant weight. Biomass is indicated as the mean ± SD of the dry weight of mycelia per unit volume of culture medium, calculated from three independent experiments.

## 2.3 Extraction and analysis of antrodin C

Antrodin C was extracted from fermentations as described<sup>24</sup> with minor modifications. Briefly, production cultures were precipitated with 50 mL of 95% ethanol in a 45°C water bath for 1.5 h with intermittent shaking. The supernatant was filtered through a 0.45 µm membrane and the concentration of antrodin C was determined by high performance liquid chromatography (HPLC) on a Waters 1525 system equipped with a ZORBAX Eclipse XDB-C18 column (4.6 mm × 250 mm, 5 µm), with the UV detector set at 254 nm. The mobile phase consisted of H<sub>2</sub>O (0.5% AcOH):CH<sub>3</sub>CN (0 min, 65:35; 10 min, 50:50; 25 min, 43:57; 50 min, 30:70; 55 min, 10:90; 60 min, 0:100; 70 min, 65:35). The flow rate was 1.0 mL/min and the operating temperature of the column was maintained at 28°C. Antrodin C yields were calculated based on the peak area using a standard curve, and are shown as the mean ± SD calculated from three independent experiments.

## 2.4 Free radical scavenging activity of antrodin C

The free radical scavenging activity of antrodin C was evaluated against 2,2'-azinobis-3-ethylbenzothiazoline-6-sulfonate radicals (ABTS<sup>•</sup>), hydroxyl radicals (OH<sup>•</sup>) and 2,2-diphenyl-1-picrylhydrazyl radicals (DPPH<sup>•</sup>). ABTS<sup>•</sup> scavenging efficiency was determined using the ABTS rapid kit (Beyotime Biotechnology, Shanghai, China) and is represented as mM Trolox-equivalent antioxidant capacity (mM TEAC). The standard curve was linear between Trolox concentrations of 0.2 mM and 1.5 mM.

The scavenging activity of antrodin C against OH<sup>•</sup> was tested according to Halliwell *et al.*<sup>26</sup>. Fifty microliters of various concentrations of the test samples were mixed with 50 µL of 6 mM ferrous sulfate and 50 µL of 6 mM H<sub>2</sub>O<sub>2</sub>. The mixture was incubated in the dark at room temperature for 10 minutes, followed by addition of 50 µL of 6 mM salicylic acid dissolved in anhydrous ethanol. The absorbance of the mixture was measured by a spectrophotometer at 510 nm. Vitamin C was used as the positive control.

The scavenging activity of antrodin C against DPPH<sup>•</sup> was monitored as previously reported<sup>27</sup>. One hundred microliters of various concentrations of the test samples were mixed with 100 µL anhydrous ethanol solution of DPPH<sup>•</sup> (0.01 mM). The mixture was

shaken and incubated in the dark at room temperature for 30 min, and the absorbance was measured using a spectrophotometer set to 517 nm. Butylated hydroxyanisole (BHA) was used as the reference.

The 50% effective concentration (EC<sub>50</sub>) for the scavenging activity against OH<sup>•</sup> or DPPH<sup>•</sup> was calculated from a linear regression curve fitted to the measured values of the scavenging activity versus substrate concentration. Radical scavenging activities are shown as the mean ± SD calculated from three independent experiments.

## 2.5 Effects of oxidative stress modulators on the production of antrodin C

Three kinds of oxidative stress inducers, including H<sub>2</sub>O<sub>2</sub>, menadione and diethyl phthalate were investigated for their effects on the production of antrodin C in submerged fermentations of *A. cinnamomea*. The concentration dependency (10, 15, 20, 25, 30 and 35 mM) and the time course (48, 72, 96, 120 and 144 hr) of H<sub>2</sub>O<sub>2</sub> supplementation were also determined.

Diphenyleneiodonium (DPI), a common inhibitor of ROS formation<sup>28</sup>, was used to investigate the role of oxidative stress to induce antrodin C biosynthesis during submerged fermentation. Pretreatment was carried out with supplementation with 1 mM DPI at 95 hr, followed by addition of H<sub>2</sub>O<sub>2</sub> at 96 hr. The electron transport chain type I complex inhibitor rotenone (7 μM, final concentration) was added to fermentations at 96 hr without H<sub>2</sub>O<sub>2</sub> induction.

## 2.6 Measurement of superoxide dismutase (SOD) and catalase (CAT) activities

0.5 g of *A. cinnamomea* mycelium was disrupted in ice-cold potassium phosphate buffer (50 mM, pH 6.8) using a pre-chilled mortar and pestle, the lysate was centrifuged at 8,000×g for 10 min at 4°C, and the pellet was discarded. Centrifugation was repeated twice more to obtain a clear supernatant. Protein concentrations were measured using the BCA kit (Sigma). The assay for CAT activity was performed as described<sup>29</sup>. SOD activity was determined by measuring the ability of the enzyme to inhibit the autoxidation of pyrogallol, measured by following the change in absorbance at 325 nm<sup>30, 31</sup>.

## 2.7 Optimization of the fermentation conditions for antrodin C production

To further enhance the production of antrodin C, different carbon sources (glucose, maltose, sucrose, rice flour, dextrin, starch), nitrogen sources (yeast peptone, yeast extract, soybean hydrolysate, ammonium sulfate, angel yeast powder, sodium nitrate), temperature (22, 25, 28, 31, 34°C) and initial pH (4, 5, 6, 7, 8), were investigated, followed by optimization of the culture conditions using the response surface method (RSM)<sup>32, 33</sup>.

## 2.8 Comparative transcriptome analysis

Transcriptome sequencing was used to compare gene expression during conventional submerged fermentation of *A. cinnamomea* with that under oxidative stress-induced maximum antrodin C production. Total RNA was extracted with the Trizol Total RNA Isolation Kit with UNIQ-10 Columns (Shanghai Sheng-Gong, China) at 216 hr of the fermentation. Total RNA concentration was determined with a Qubit 2.0 fluorometer

(Invitrogen), and its quality was ascertained by agarose gel electrophoresis. Total RNA samples extracted from three biological replicates were mixed in equal proportions and sequenced using Illumina HiSeq™ 2500 technology by the Sheng-Gong Biotechnology Corporation (Shanghai, China). After removing linker sequences and low-quality bases (Q value <20), a 5 bp sliding window was used to identify and delete the bases with a read tail mass value of <20. Finally, reads shorter than 35 nt were discarded, and the remaining reads were used in the assembly. Next, 10,000 reads were randomly extracted from the cleaned dataset and compared to the NCBI nucleotide database using blastn to determine species distribution and thereby detect contamination, using a cutoff e-value  $\leq 1e-10$ , similarity >90% and coverage >80%. *De novo* contig assembly was completed using Trinity<sup>34</sup> (Parameter min\_kmer\_cov 2, others as defaults), redundant contigs were clustered and the longest contigs in the clusters were used to create a Unigene transcript database. Differentially expressed genes (DEGs) were identified by DEseq (qValue<0.05 and difference multiple |FoldChange|>2)<sup>35, 36</sup>, annotated using the Conserved Domain Database (CDD), the euKaryotic Ortholog Groups (KOG), the Clusters of Orthologous Groups of proteins, and the NCBI non-redundant protein sequences. Additionally, gene ontology (GO) was determined using the Uniprot annotation information based on Wisprot and TrEMBL, and Kyoto Encyclopedia of Genes and Genomes (KEGG) annotations were also gathered using the KEGG Automated Annotation Server<sup>35, 37</sup>. Annotations were followed by clustering analysis. Last, Cluster Profiler was used to analyze the KEGG pathway and KOG classification enrichment of the DEGs and to map the network based on the results of gene function enrichment analysis<sup>35</sup>.

## 2.9 Verification of the relationship between the electron transport chain and antrodin C biosynthesis

In previous studies, Chen *et al.*, showed that supplementation of mitochondrial electron transport chain type I complex inhibitors, such as rotenone, could significantly increase the level of ROS in cells<sup>38</sup>. To further validate the conclusions of the transcriptome analysis, rotenone was added to *A. cinnamomea* fermentations without H<sub>2</sub>O<sub>2</sub> induction, and the biomass and the production of antrodin C were determined at the end of the fermentation in three independent experiments.

## 3. Result and discussion

### 3.1 Free radical scavenging activity of antrodin C

To evaluate antrodin C as an antioxidant, the *in vitro* radical scavenging activity of this SM was investigated against radicals of 2,2'-azinobis-3-ethylbenzothiazoline-6-sulfonate (ABTS<sup>•</sup>), hydroxyl (OH<sup>•</sup>) and 2,2-diphenyl-1-picrylhydrazyl (DPPH<sup>•</sup>). As shown in Table 1, the ABTS<sup>•</sup> scavenging activity of antrodin C was weaker than those of well-recognized antioxidants such as vitamin C, vitamin E, or glutathione. However, antrodin C displayed potent OH<sup>•</sup> scavenging activity with a 50% effective concentration (EC<sub>50</sub>) of 0.79 mg/mL, similar to vitamin E or glutathione, but approximately 50% of that of the control vitamin C (0.37 mg/mL). Finally, antrodin C displayed a more potent scavenging activity (EC<sub>50</sub> of 0.0015 mg/mL) against DPPH<sup>•</sup> than the positive control, butylated hydroxyanisole (BHA,



EC<sub>50</sub> of 0.0034 mg/mL). Thus, antrodin C was confirmed to be an antioxidant SM of *A. cinnamomea* with a sizeable free radical scavenging potential.

### 3.2 Oxidative stress reagents increase antrodin C biosynthesis

Various reagents that induce oxidative stress during submerged fermentation affect the growth rate and biomass accumulation of microorganisms, and modulate their production of SMs<sup>3, 13, 28, 39, 40</sup>. Considering the antioxidant and free radical scavenging activities of antrodin C, we hypothesized that supplementation of *A. cinnamomea* fermentations with oxidative stress inducers may provoke this fungus to upregulate the biosynthesis of antrodin C. To evaluate this hypothesis, we applied diethyl phthalate (a toxic compound that elevates intracellular ROS levels), menadione (a producer of semiquinone and superoxide radicals) and H<sub>2</sub>O<sub>2</sub> (a microbicidal oxidizing agent)<sup>41–44</sup> during *A. cinnamomea* fermentations at the stage when antrodin C accumulation starts (96 hr), and determined biomass production and antrodin C yield at the end of the fermentation (216 hr).

We found that with increased concentrations of any of the three oxidative stress reagents, mycelial pellet size and biomass accumulation of *A. cinnamomea* slightly but steadily declined, indicating that these reagents function as weak inhibitors of fungal growth (Fig. 1). At the same time, the three oxidative stress inducers stimulated the biosynthesis of antrodin C, with optimal concentrations for H<sub>2</sub>O<sub>2</sub>, menadione and diethyl phthalate at 25 mM, 7 μM and 1 mM, respectively. Increased concentrations of the oxidative stress inducers led to a progressive decline of antrodin C production. Lower concentrations of these reagents may have induced insufficient oxidative stress, with ROS effectively detoxified by intracellular antioxidant enzymes such as superoxide dismutase (SOD) and catalase (CAT) before they could affect the expression of key genes in antrodin C biosynthesis in *A. cinnamomea*.

The most effective oxidative stress inducer to improve antrodin C biosynthesis was H<sub>2</sub>O<sub>2</sub>. At the optimum concentration of 25 mM, the yield of antrodin C reached 361.5 ± 11.15 mg/L, representing an increase of 4.8 times over that of the control fermentations (Fig. 1). Therefore, H<sub>2</sub>O<sub>2</sub> was used as the oxidative stress elicitor in further experiments.

The timing of H<sub>2</sub>O<sub>2</sub> supplementation was found to be critical for biomass accumulation and the stimulation of antrodin C production in the submerged *A. cinnamomea* fermentations. As shown in Fig. 1D, inhibition of biomass accumulation by H<sub>2</sub>O<sub>2</sub> became less apparent when supplementation of this oxidative stress inducer was delayed. On the other hand, the antrodin C yield-enhancing effect of H<sub>2</sub>O<sub>2</sub> showed a clear maximum when the supplementation was timed to coincide with the start of antrodin C accumulation at 96 hr. This suggests that H<sub>2</sub>O<sub>2</sub>-generated oxidative stress is most effective when the transcription of antrodin C biosynthetic genes is the most active.

### 3.3 Intracellular ROS generation directly affects antrodin C biosynthesis

Next, we have used diphenyleneiodonium (DPI; an inhibitor of mitochondrial ROS production<sup>45</sup>) to clarify whether H<sub>2</sub>O<sub>2</sub> elicits the production of antrodin C *via* enhancing the level of intracellular ROS in *A. cinnamomea*. DPI was supplemented to the cultures at 95 hr, followed by addition of H<sub>2</sub>O<sub>2</sub> at 96 hr. DPI supplementation alone had no effect on biomass accumulation or antrodin C production in this fungus. H<sub>2</sub>O<sub>2</sub> supplementation reduced

biomass accumulation as expected, and this decrease was not alleviated by the addition of DPI. However, the sizeable increase of antrodin C production due to H<sub>2</sub>O<sub>2</sub> supplementation was completely negated by the co-administration of DPI (Fig. 2). We conclude that DPI effectively inhibited intracellular ROS generation and thereby counteracted the effects of H<sub>2</sub>O<sub>2</sub> towards antrodin C biosynthesis. This result establishes a tight correlation among oxidative stress caused by H<sub>2</sub>O<sub>2</sub>, intracellular ROS production, and increased antrodin C biosynthesis.

Antioxidant enzyme systems including SOD and CAT act as the first line of defense against increased ROS levels to protect the intracellular environment. To further confirm intracellular ROS-mediated oxidative stress upon H<sub>2</sub>O<sub>2</sub> supplementation, we monitored the activity of SOD and CAT during the fermentation. As shown in Fig. 3a and b, both SOD and CAT activities increased when H<sub>2</sub>O<sub>2</sub> was supplemented to the cultures, reaching peak activities that were 1.30 and 1.35 times of that of the control, respectively. SOD activity remained very high even in the later stages of fermentation in the H<sub>2</sub>O<sub>2</sub>-supplemented cultures, while that in the control decreased steadily. Addition of DPI blocked the increase in both enzyme activities, indicating that DPI effectively inhibited the H<sub>2</sub>O<sub>2</sub>-provoked generation of intracellular ROS.

To gain a perspective on the short-term effects of H<sub>2</sub>O<sub>2</sub> addition on the CAT and SOD activity of the cells, we also monitored the changes in these enzyme activities in the first 180 min after the addition of H<sub>2</sub>O<sub>2</sub> (Fig. 3c). SOD activity peaked within 60 min and then declined, while CAT activity showed a much slower response time (reaching the maximum at 150 min). This may be attributed to a sequence of events where SOD first catalyzes superoxide anion radical disproportionation to form oxygen and H<sub>2</sub>O<sub>2</sub>, and this is followed by CAT converting H<sub>2</sub>O<sub>2</sub> to oxygen<sup>46, 47</sup>. The results indicated that the addition of H<sub>2</sub>O<sub>2</sub> not only causes a change in the intracellular ROS content, but also produces more than one type of ROS for stimulating the biosynthesis of antrodin C.

### 3.4 Process optimization of antrodin C production during H<sub>2</sub>O<sub>2</sub>-provoked oxidative stress

Nutrients and culture conditions are critical factors for microbial growth and the biosynthesis of SMs that need to be re-optimized following significant changes in the fermentation process, such as the introduction of oxidative stress inducers to the medium<sup>48,49</sup>. Thus, we systematically investigated different kinds of carbon and nitrogen sources, growth temperatures, and the initial pH on antrodin C production during submerged fermentation of *A. cinnamomea* in the presence of H<sub>2</sub>O<sub>2</sub> (Fig. 4). The tested factors all exerted significant influence on both biomass accumulation and the production of antrodin C. Our results showed that the optimal antrodin C-producing conditions under H<sub>2</sub>O<sub>2</sub> stress are as follows: maltose 50 g/L, soybean hydrolysate 60 mL/L, temperature 25°C, initial pH 7, and H<sub>2</sub>O<sub>2</sub> supplementation to 25 mM at 96 hr. Under these conditions, the yield of antrodin C reached 594.4 mg/L at 216 hr, corresponding to a 352.1% increase over the standard conditions without H<sub>2</sub>O<sub>2</sub> stress (131.5 mg/L). Next, we completed a three-factor and three-level response surface optimization experiment. A summary of the variables and their variation levels, results from parameter optimization with a Box–Behnken design and analysis of the results are displayed in Supporting Information (SI) Table S1. The analysis of



variance was employed for the determination of significant parameters, and allowed us to derive a model equation fitted by regression analysis as:

$$[\text{Antrocin C}] = 604.29 + 4.07775X_1 - 17.3049X_2 - 3.88981X_3 + 12.03313X_1X_2 - 9.55638X_1X_3 - 5.40075X_2X_3 - 89.6255X_1^2 - 44.5059X_2^2 - 67.7614X_3^2$$

The model reliability was confirmed by the P-value of <0.0001, the model determination coefficient of  $R^2=0.9983$  and the significance of the residual (0.1906). The single factors  $X_1$ , ( $\text{H}_2\text{O}_2$ ),  $X_2$ , (temperature),  $X_3$ , (initial pH), and the interaction factors  $X_1X_2$ ,  $X_1X_3$ ,  $X_2X_3$ ,  $X_1^2$ ,  $X_2^2$  and  $X_3^2$  were proven to be significant. The fitted response surface for antrocin C production, generated using the software Origin with this model shows the effects of interaction between the three critical parameters,  $\text{H}_2\text{O}_2$  concentration, temperature, and initial pH, respectively (SI Table S1). The strength rank of the interactions was  $X_1X_2 > X_1X_3 > X_2X_3$ . Based on the response surface analysis of this mathematical model, the optimal culture conditions were determined as  $\text{H}_2\text{O}_2$  concentration of 25 mM, culture temperature of 24°C, and initial pH of 7. Under these optimal conditions, the maximal production of antrocin C reached 605.1 mg/L, 7.9 times as high as that of the control in this experiment (77.0 mg/L without  $\text{H}_2\text{O}_2$  induction).

### 3.5 Transcriptomic analysis of $\text{H}_2\text{O}_2$ stress

To better investigate the molecular mechanism of  $\text{H}_2\text{O}_2$  elicitation of antrocin C production in *A. cinnamomea*, we used RNA-seq analysis to compare the transcriptome of the antrocin C-overproducing,  $\text{H}_2\text{O}_2$ -stressed culture with that of the control fermentation without oxidative stress. As show in SI Table S2A, mapping rates were over 94%, indicating that the sequence data were highly accurate. A total of 120,623 transcripts, 34,512 Unigenes (SI Tables S2B) and 22,486 proteins were obtained after *de novo* assembly and annotation. The expression levels of genes in the two samples were compared using Transcript Per Million reads (TPM) as the measure. The intra-group differences were much less than the difference between the control and the  $\text{H}_2\text{O}_2$ -elicited sample (SI Fig. S1). Using filter conditions of  $q\text{Value} < 0.05$  and  $|\text{FoldChange}| > 2$ , 317 differentially expressed genes (DEGs) were identified (SI Table S3A). These DEGs were annotated using their Gene Ontology (GO), Kyoto Encyclopedia of Genes and Genomes (KEGG) and Eukaryotic Orthologous Groups (KOG) classifications (Fig. 5 and SI Tables S3B, S3C and S3D).

Upregulated DEGs were found by GO analysis in the glutathione peroxidase family, polyketide metabolism, *O*-methyltransferases, heterocyclic biosynthesis and decomposition processes, and heterocyclic compound binding classes. On the other hand, downregulated DEGs were prominent in the electron transport chain, tricarboxylic acid cycle, citrate (Si)-synthase activity, ubiquinol-cytochrome-c reductase activity, NADH dehydrogenase (ubiquinone) activity and mitochondrial ATP synthesis coupled electron transport groups. KEGG pathway analysis revealed that DEGs were significantly enriched in metabolic and signal transduction pathways, and many downregulated DEGs were linked with oxidative phosphorylation. Similarly, KOG analysis showed that many significantly downregulated DEGs are involved in energy production and conversion.

Regrettably, a direct analysis of the antrodin C biosynthetic genes could not be completed since the biosynthetic pathway for this SM remains uncharacterized. Based on literature precedents of maleimide biosynthesis in *Penicillium oxalicum*<sup>50</sup>, we tentatively identified six genes in the transcriptome of *A. cinnamomea* that may be involved in antrodin formation in *A. cinnamomea*. Several of these transcripts were found to be upregulated upon H<sub>2</sub>O<sub>2</sub> supplementation (SI Table S4). Functional validation of the role(s), if any, of the corresponding genes in antrodin C biosynthesis in *A. cinnamomea* is currently under way in our laboratories.

Overall, H<sub>2</sub>O<sub>2</sub> supplementation led to a significant activation of the transcription of genes related to catabolism and antioxidant processes, and to the overall repression of the tricarboxylic acid cycle and the electron transport chain. Remarkably, many downregulated DEGs are involved in oxidative phosphorylation (Table 2)<sup>51</sup>, indicating that increased biosynthesis of antrodin C upon H<sub>2</sub>O<sub>2</sub>-provoked ROS stress has an underlying link with the electron transport chain. Considering that electron leakage from the mitochondrial electron transport system is one of the main sources of ROS production in microorganisms<sup>44, 52</sup> and microbial metabolism also can be regulated by controlling the electron transport chain<sup>53</sup>, we propose that mitochondrial respiratory chain damage caused by H<sub>2</sub>O<sub>2</sub> stress leads to elevated ROS production, which increased production of antioxidant metabolites such as antrodin C.

### 3.6 Verification of the transcriptomic study by supplementing rotenone to the fermentation

To validate the relationship between the health of the mitochondrial electron transport chain and the biosynthesis of antrodin C as suggested by our comparative transcriptomic study, we selected rotenone to disturb the normal course of oxidative phosphorylation in *A. cinnamomea* fermentations. Rotenone inhibits the transfer of electrons from NADH to coenzyme Q *via* decreasing the activity of complex I, leading to the generation of ROS<sup>38</sup>. We found that supplementation of different concentrations of rotenone affected the biosynthesis of antrodin C without disturbing biomass accumulation (Fig. 6). The yield of antrodin C reached  $200.8 \pm 14.97$  mg/L when 7  $\mu$ M rotenone was added to the cultures, representing an increase of 2.6 times over that of the control. Thus, a direct disruption of the mitochondrial electron transport chain by rotenone mimics the effects of the oxidative stress generated by H<sub>2</sub>O<sub>2</sub> on the biosynthesis of antrodin C.

### 3.7 Conclusions

This study illustrates a rational approach that utilizes a metabolic stressor to provoke the increased biosynthesis of an SM that the producer cells use to restore homeostasis. Thus, H<sub>2</sub>O<sub>2</sub> is an oxidative stress inducer that effectively stimulates the biosynthesis of the *A. cinnamomea* antioxidant antrodin C, a valuable SM with potential applications in pharmaceutical drug discovery. Further research is still necessary to understand the effects of oxidative stress on the biosynthesis of antrodin C and similar secondary metabolites in fungi. In particular, although we could successfully use DPI supplementation to counteract the positive effects of H<sub>2</sub>O<sub>2</sub> on the production of antrodin C and to block the increase in the activity of antioxidant enzymes, there are some doubts about the specificity of DPI as an inhibitor of intracellular ROS generation. Thus, Aldieri *et al.*<sup>54</sup> suggested that DPI should

not be used as a specific NOX inhibitor. To allay such concerns, we plan to use and combine multiple ROS inhibitors such as *N*-acetyl-L-cysteine and vitamin C<sup>55,56</sup> in our follow-up work, and we will also consider monitoring intracellular ROS levels by fluorescent staining<sup>57</sup>. We also are in the process of validating potential antrodin C biosynthetic genes using qRT-PCR, gene knockout/knockdown and overexpression studies. Elucidation of the chain of events that connects H<sub>2</sub>O<sub>2</sub>-induced oxidative damage, disturbance of mitochondrial electron transport, increased ROS formation and the activation of antrodin C biosynthetic genes will help to fine-tune fermentation process improvement strategies for the production of antrodin C and other antioxidant metabolites.

## Supplementary Material

Refer to Web version on PubMed Central for supplementary material.

## Acknowledgments

### Funding sources

This work was supported by the National Key Research and Development Program of China (2016YFD0400802), the Natural Science Foundation of Jiangsu Province (BK20181348), the Six Talent Peak Project of Jiangsu Province (SWYY-211), the national first-class discipline program of Light Industry Technology and Engineering (LITE2018-08), the USDA National Institute of Food and Agriculture Hatch project (1020652 to I.M.); the Higher Education Institutional Excellence Program of the Ministry of Human Capacities in Hungary (20428-3/2018/FEKUTSTRAT to I.M.); and the U.S. National Institutes of Health (NIGMS 5R01GM114418 to I.M.).

## Reference

1. Zhang BB; Hu PF; Huang J; Hu YD; Chen L; Xu GR Current advances on the structure, bioactivity, synthesis, and metabolic regulation of novel ubiquinone derivatives in the edible and medicinal mushroom *Antrodia cinnamomea*. *J. Agric. Food Chem* 2017, 65, 10395–10405. [PubMed: 29125753]
2. Wasser SP Medicinal mushrooms in human clinical studies. part I. anticancer, oncoimmunological, and immunomodulatory activities: a review. *Int. J. Med. Mushrooms* 2017, 19, 279–317. [PubMed: 28605319]
3. Yan G; Hua Z; Liu D; Du G; Chen J Influence of oxygen level on oxidative stress response of *Bacillus* sp. F26 to menadione. *Process Biochem.* 2006, 41, 764–769.
4. Liou GY; Storz P Reactive oxygen species in cancer. *Free Radical Res.* 2010, 44, 479–496. [PubMed: 20370557]
5. Aguirre J; Mauricio RM; Hewitt D; Hansberg W Reactive oxygen species and development in microbial eukaryotes. *Trends Microbiol.* 2005, 13, 111–118. [PubMed: 15737729]
6. Angelova MB; Pashova SB; Spasova BK; Vassilev SV; Slokoska LS Oxidative stress response of filamentous fungi induced by hydrogen peroxide and paraquat. *Mycol Res.* 2005, 109, 150–158. [PubMed: 15839099]
7. Han PP; Shen SG; Guo RJ; Zhao DX; Lin YH; Jia SR; Yan RR; Wu YK ROS is a factor regulating the increased polysaccharide production by light quality in the edible cyanobacterium *Nostoc flagelliforme*. *J. Agric. Food Chem* 2019, 67, 2235–2244. [PubMed: 30724068]
8. Beracochea VC; Almasia NI; Peluffo L; Nahirñak V; Hopp E; Paniego N; Heinz RA; Vazquez-Rovere C; Lia VV Sunflower germin-like protein HaGLP1 promotes ROS accumulation and enhances protection against fungal pathogens in transgenic *Arabidopsis thaliana*. *Plant Cell Rep.* 2015, 34, 1717–1733. [PubMed: 26070410]
9. Ren A; Liu R; Miao ZG; Zhang X; Cao PF; Chen TX; Li CY; Shi L; Jiang AL; Zhao MW Hydrogen-rich water regulates effects of ROS balance on morphology, growth and secondary

- metabolism via glutathione peroxidase in *Ganoderma lucidum*. *Environ. Microbiol* 2017, 19,566–583. [PubMed: 27554678]
10. Sun Q; Shang B; Wang L; Lu Z; Liu Y Cinnamaldehyde inhibits fungal growth and aflatoxin B biosynthesis by modulating the oxidative stress response of *Aspergillus flavus*. *Appl. Microbiol. Biot* 2016, 100, 1355–1364.
  11. Shi L; Gong L; Zhang X; Ren A; Gao T; Zhao M The regulation of methyl jasmonate on hyphal branching and GA biosynthesis in *Ganoderma lucidum* partly via ROS generated by NADPH oxidase. *Fungal Genet. Biol* 2015, 81, 201–211. [PubMed: 25512263]
  12. Montibus M; Pinson-Gadais L; Richard-Forget F; Barreau C; Ponts N Coupling of transcriptional response to oxidative stress and secondary metabolism regulation in filamentous fungi. *Crit. Rev. Microbiol* 2013, 41, 295–308. [PubMed: 24041414]
  13. Wang HB; Luo J; Huang XY; Lu MB; Yu LJ Oxidative stress response of *Blakeslea trispora* induced by H<sub>2</sub>O<sub>2</sub> during  $\beta$ -carotene biosynthesis. *J. Ind. Microbiol. Biot* 2014, 41, 555–561.
  14. Geethangili M; Tzeng YM Review of pharmacological effects of *Antrodia camphorata* and its bioactive compounds. *Evid. Based Complement Alternat. Med* 2011, 212641.
  15. Chen PY; Wu JD; Tang KY; Yu CC; Kuo YH; Zhong WB; Lee CK Isolation and synthesis of a bioactive benzenoid derivative from the fruiting bodies of *Antrodia camphorata*. *Molecules* 2013, 18, 7600–7608. [PubMed: 23812251]
  16. Hsu YL; Kuo YC; Kuo PL; Ng LT; Kuo YH; Lin CC Apoptotic effects of extract from *Antrodia camphorata* fruiting bodies in human hepatocellular carcinoma cell lines. *Cancer Lett.* 2005, 221, 77. [PubMed: 15797630]
  17. Senthil KKJ; Vani GM; Wang SY Activation of Nrf2-mediated anti-oxidant genes by antrodin C prevents hyperglycemia-induced senescence and apoptosis in human endothelial cells. *Oncotarget.* 2017, 8, 96568–96587. [PubMed: 29228553]
  18. Chien SC; Chen ML; Kuo HT; Tsai YC; Lin BF; Kuo YH Anti-inflammatory activities of new succinic and maleic derivatives from the fruiting body of *Antrodia camphorata*. *J. Agric. Food Chem* 2008, 56, 7017–22. [PubMed: 18642845]
  19. Kumar KJ; Vani MG; Chueh PJ; Mau JL; Wang SY Antrodin C inhibits epithelial-to-mesenchymal transition and metastasis of breast cancer cells via suppression of Smad2/3 and  $\beta$ -catenin signaling pathways. *Plos One.* 2015, 10, e0117111. [PubMed: 25658913]
  20. Phuong DT; Ma CM; Hattori M; Jin JS Inhibitory effects of antrodins A-E from *Antrodia cinnamomea* and their metabolites on hepatitis C virus protease. *Phytotherapy Research Ptr.* 2009, 23, 582–584. [PubMed: 19003946]
  21. Nakamura N; Hirakawa A; Gao JJ; Kakuda H; Shiro M; Komatsu Y; Sheu CC; Hattori M Five new maleic and succinic acid derivatives from the mycelium of *Antrodia camphorata* and their cytotoxic effects on LLC tumor cell line. *J. Nat. Prod* 2004, 67, 46–48. [PubMed: 14738384]
  22. Yang H; Bai X; Zhang H; Zhang J; Wu Y; Tang C; Liu Y; Yang Y; Liu Z; Jia W, Antrodin C, an NADPH dependent metabolism, encourages crosstalk between autophagy and apoptosis in lung carcinoma cells by use of an AMPK inhibition-independent blockade of the Akt/mTOR pathway. *Molecules* 2019, 24, 993.
  23. Wang W; Yang H; Deng J; Zhu L; Yang Y; Liu Z; Zhang JS; Tang C; Zhang Z; Zhuang H Increased inhibition effect of antrodin C from the stout camphor medicinal mushroom, *Taiwanofungus camphoratus* (Agaricomycetes), on A549 through crosstalk between apoptosis and autophagy. *Int. J. Med. Mushr* 2019, 21, 595–610.
  24. Zhang H; Xia YJ; Wang YL; Zhang BB; Xu GR Coupling use of surfactant and in situ extractant for enhanced production of Antrodin C by submerged fermentation of *Antrodia camphorata*. *Biochem. Eng. J* 2013, 79, 194–199.
  25. Hu YD; Lu RQ; Liao XR; Zhang BB; Xu GR Stimulating the biosynthesis of Antroquinonol by addition of effectors and soybean oil in submerged fermentation of *Antrodia camphorata*. *J. Appl. Biochem* 2016, 63, 398–406.
  26. Halliwell B; Gutteridge JM; Aruoma OI The deoxyribose method: a simple “test-tube” assay for determination of rate constants for reactions of hydroxyl radicals. *Anal. Biochem* 1987, 165, 215–219. [PubMed: 3120621]

27. Hsiao G; Shen MY; Lin KH; Lan MH; Wu LY; Chou DS; Lin CH; Su CH; Sheu JR Antioxidative and hepatoprotective effects of *Antrrodia camphorata* extract. *J. Agric. Food Chem* 2003, 51, 3302–3308. [PubMed: 12744658]
28. Wei ZH; Bai L; Deng Z; Zhong JJ Enhanced production of validamycin A by H<sub>2</sub>O<sub>2</sub>-induced reactive oxygen species in fermentation of *Streptomyces hygroscopicus* 5008. *Bioresour. Technol* 2011, 102, 1783–1787. [PubMed: 20952185]
29. Weydert CJ; Cullen JJ Measurement of superoxide dismutase, catalase and glutathione peroxidase in cultured cells and tissue. *Nat. Protoc* 2010, 5, 51–66. [PubMed: 20057381]
30. Sandström BE; Granström M; Vezin H; Bienvenu P; Marklund SL A comparison of four assays detecting oxidizing species. Correlated reactivity of Fe(III)-quin2, but not Fe(III)-EDTA, with hydrogen peroxide. *Biol. Trace Elem. Res* 1995, 47, 29–36. [PubMed: 7779560]
31. Reddy PY; Giridharan NV; Reddy GB Activation of sorbitol pathway in metabolic syndrome and increased susceptibility to cataract in wistar-obese rats. *Mol. Vis* 2012, 18, 495. [PubMed: 22393276]
32. Tanyildizi MS; Elibol OM Optimization of  $\alpha$ -amylase production by *Bacillus* sp. using response surface methodology. *Process Biochem.* 2005, 40, 2291–2296.
33. Najafi B; Ardabili SF; Mosavi A; Shamshirband S; Rabczuk T An intelligent artificial neural network-response surface methodology method for accessing the optimum biodiesel and diesel fuel blending conditions in a diesel engine from the viewpoint of exergy and energy analysis. *Energies* 2018, 11, 860.
34. Eccles D; Chandler J; Camberis M; Henrissat B; Koren S; Le Gros G; Ewbank JJ De novo assembly of the complex genome of *Nippostrongylus brasiliensis* using MinION long reads. *BMC biology.* 2018, 16, 6. [PubMed: 29325570]
35. Liu W; Li L; Long X; You W; Zhong Y; Wang M; Tao H; Lin S; He H Construction and analysis of gene co-expression networks in *Escherichia coli*. *Cells* 2018, 7, 19.
36. Yu L; Tie shan F; Li L; Chen S; Xiao LL Comparative analysis of molecular aberration in different genders for identification of key pathways in hepatocellular carcinoma. *American Society Clin. Oncol* 2019.
37. Li HX; Lu ZM; Zhu Q; Gong JS; Geng Y; Shi JS; Xu ZH; Ma YH Comparative transcriptomic and proteomic analyses reveal a FluG-mediated signalling pathway relating to asexual sporulation of *Antrrodia camphorata*. *Proteomics* 2017, 17.
38. Chen Y; McMillan-Ward E; Kong J; Israels SJ; Gibson SB Mitochondrial electron-transport-chain inhibitors of complexes I and II induce autophagic cell death mediated by reactive oxygen species. *J. Cell Sci* 2007, 120, 4155–4166. [PubMed: 18032788]
39. Miranda RU; Gómez-Quiroz LE; Mejía A; Barrios-González J Oxidative state in idiophase links reactive oxygen species (ROS) and lovastatin biosynthesis: Differences and similarities in submerged and solid-state fermentations. *Fung. Biol* 2013, 117, 85–93.
40. Miranda RU; Gómez-Quiroz LE; Mendoza M; Pérez-Sánchez A; Fierro F; Barrios-González J Reactive oxygen species regulate lovastatin biosynthesis in *Aspergillus terreus* during submerged and solid-state fermentations. *Fung. Biol* 2014, 118, 979–989.
41. Kreiner M; Harvey LM; Mc NB Oxidative stress response of a recombinant *Aspergillus niger* to exogenous menadione and H<sub>2</sub>O<sub>2</sub> addition. *Enzyme Microb. Technol* 2002, 30, 346–353.
42. Steinmeier J; Dringen R Exposure of cultured astrocytes to menadione triggers rapid radical formation, glutathione oxidation and mrp1-mediated export of glutathione disulfide. *Neurochem. Res* 2019, 1–15.
43. Yu J; Yang C; Yu R; Fu G Toxic response of dimethyl phthalate (DMP) to *Gracilaria lemaneiformis*. *Electronic J. Biol* 2007, 3, 80–86.
44. Liu R; Cao P; Ren A; Wang S; Yang T; Zhu T; Shi L; Zhu J; Jiang AL; Zhao MW SA inhibits complex III activity to generate reactive oxygen species and thereby induces GA overproduction in *Ganoderma lucidum*. *Redox Biol.* 2018, 16, 388–400. [PubMed: 29631100]
45. Lambert AJ; Buckingham JA; Boysen HM; Brand MD Diphenyleneiodonium acutely inhibits reactive oxygen species production by mitochondrial complex I during reverse, but not forward electron transport. *Biochim. Biophys. Acta* 2008, 1777, 397–403. [PubMed: 18395512]

46. Ighodaro OM; Akinloye OA First line defence antioxidants-superoxide dismutase (SOD), catalase (CAT) and glutathione peroxidase (GPX): Their fundamental role in the entire antioxidant defence grid. *Alexandria J. Med* 2017, S2090506817301550.
47. Azarabadi S; Abdollahi H; Torabi M; Salehi Z; Nasiri J ROS generation, oxidative burst and dynamic expression profiles of ROS-scavenging enzymes of superoxide dismutase ( SOD ), catalase ( CAT ) and ascorbate peroxidase ( APX ) in response to *Erwinia amylovora* in pear ( *Pyrus communis* L). *Eur. J. Plant Pathol* 2017, 147, 279–294.
48. Xia Y; Wang Y; Zhang B; Xu G; Ai L Effect of cultural conditions on antrodin C production by basidiomycete *Antrodia camphorata* in solid-state fermentation. *Biotechnol. Appl. Biochem* 2014, 61, 724–732. [PubMed: 24548184]
49. Shih IL; Tsai KL; Hsieh C Effects of culture conditions on the mycelial growth and bioactive metabolite production in submerged culture of *Cordyceps militaris*. *Biochem. Eng. J* 2006, 33, 193–201.
50. Sato M; Dander JE; Sato C; Hung YS; Gao SS; Tang MC; Hang L; Winter JM; Garg NK; Watanabe K 2017. Collaborative biosynthesis of maleimide- and succinimide-containing natural products by fungal polyketide megasynthases. *J. Am. Chem. Soc* 2017, 139, 5317–5320. [PubMed: 28365998]
51. Nath S Analysis of molecular mechanisms of ATP synthesis from the standpoint of the principle of electrical neutrality. *Biophys. Chem* 2017, 224, 49–58. [PubMed: 28318906]
52. Baldissera MD; Souza CF; Grings M; Parmeggiani BS; Leipnitz G; Moreira KL; da Rocha MIU; da Veiga ML; Santos RC; Stefani LM Inhibition of the mitochondrial respiratory chain in gills of *Rhamdia quelen* experimentally infected by *Pseudomonas aeruginosa*: Interplay with reactive oxygen species. *Microb. Pathogenesis*. 2017, 107, 349–353.
53. Wu H; Tuli L; Bennett GN; San KY Metabolic transistor strategy for controlling electron transfer chain activity in *Escherichia coli*. *Meta. Eng* 2015, 28, 159–168.
54. Aldieri E; Riganti C; Polimeni M; Gazzano E; Lussiana C; Campia I; Ghigo D Classical inhibitors of NOX NAD (P) H oxidases are not specific. *Curr. Drug. Metab* 2008, 9, 686–696. [PubMed: 18855607]
55. Halasi M; Wang M; Chavan TS; Gaponenko V; Hay N; Gartel AL, ROS inhibitor N-acetyl-L-cysteine antagonizes the activity of proteasome inhibitors. *Biochem. J* 2013, 454, 201–208. [PubMed: 23772801]
56. Sang X; Wang H; Chen Y; Guo Q; Lu A; Zhu X; Meng G, Vitamin C inhibits the activation of the NLRP3 inflammasome by scavenging mitochondrial ROS. *Inflammasome* 2016, 2.
57. Liu R; Cao P; Ren A; Wang S; Yang T; Zhu T; Shi L; Zhu J; Jiang AL; Zhao MW SA inhibits complex III activity to generate reactive oxygen species and thereby induces GA overproduction in *Ganoderma lucidum*. *Redox. Biol* 2018, 16, 388–400. [PubMed: 29631100]



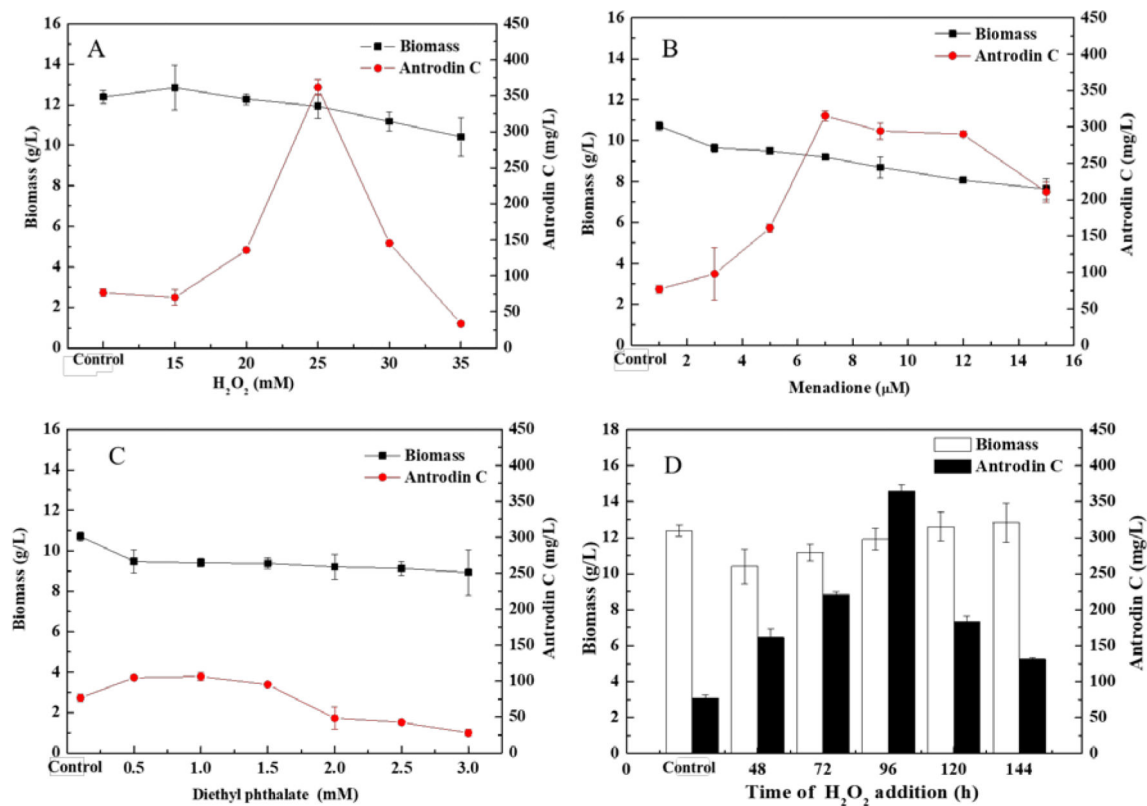


**Fig 1. Effects of oxidative stress inducers on the biomass accumulation and the production of antrodin C in *A. cinnamomea*.**

Submerged fermentations were supplemented at 96 hr with the indicated concentrations of: a, hydrogen peroxide (H<sub>2</sub>O<sub>2</sub>); b, menadione; c, diethyl phthalate. d, Time course of the addition of 25 mM H<sub>2</sub>O<sub>2</sub> to *A. cinnamomea* fermentations. Data are the mean ± SD calculated from three independent experiments.

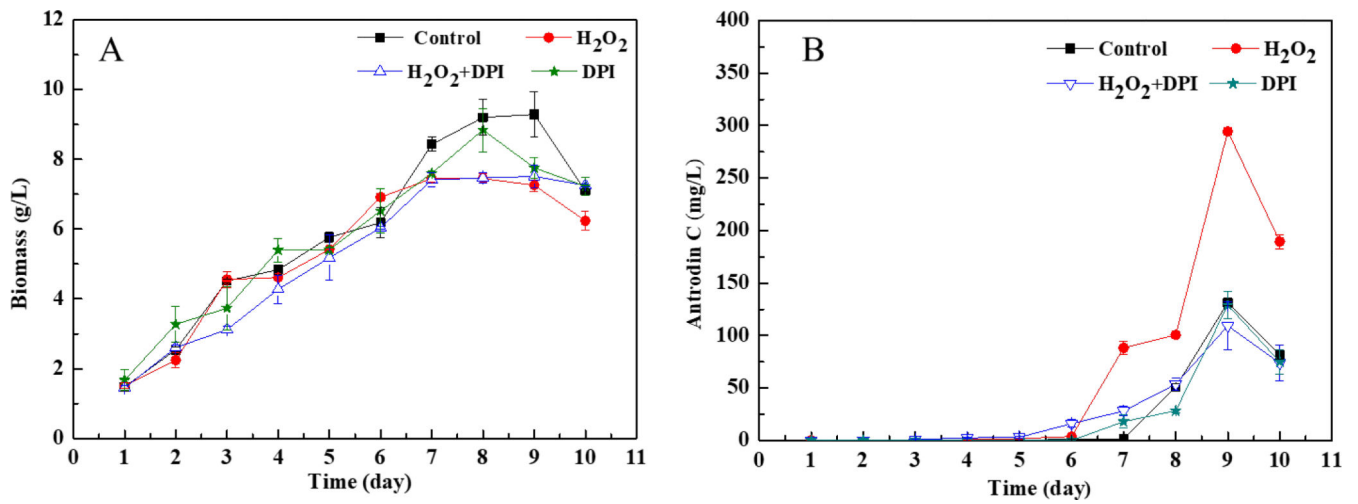


**Fig 2. Effects of H<sub>2</sub>O<sub>2</sub> and/or diphenyleneiodonium (DPI) on the biomass accumulation and the production of antrodin C in *A. cinnamomea*.**

DPI (1 mM, final concentration) was added at 95 hr, while H<sub>2</sub>O<sub>2</sub> (25 mM, final concentration) was supplemented at 96 hr. Biomass concentrations (a) and antrodin C yields (b) are shown as the mean  $\pm$  SD calculated from three independent experiments.

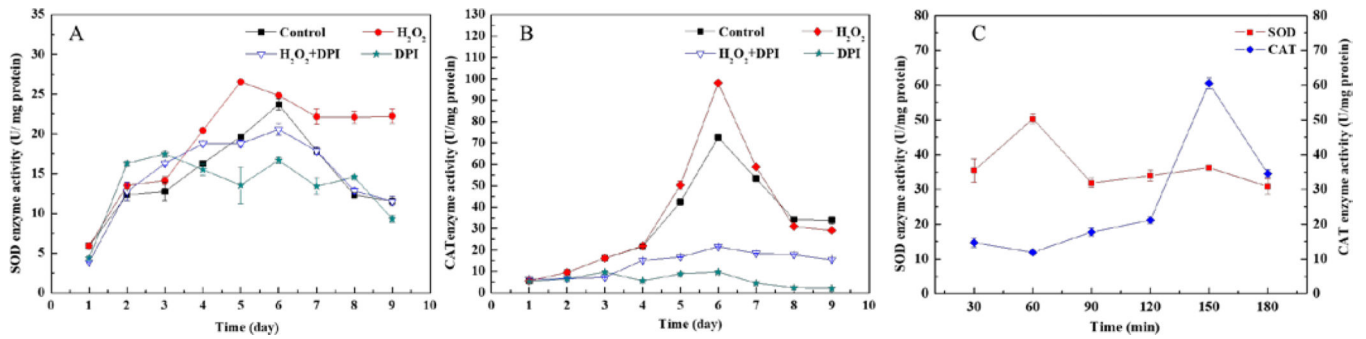


**Fig 3.** Effect of H<sub>2</sub>O<sub>2</sub> and/or DPI on the intracellular SOD and CAT activities of *A. cinnamomea*. DPI (1 mM, final concentration) was added at 95 hr, while H<sub>2</sub>O<sub>2</sub> (25 mM, final concentration) was supplemented at 96 hr. SOD (a) and CAT (b) activities during the full course of the *A. cinnamomea* fermentation, or both enzyme activities during the first 180 min following H<sub>2</sub>O<sub>2</sub> supplementation are shown as the mean specific activity  $\pm$  SD calculated from three independent experiments.

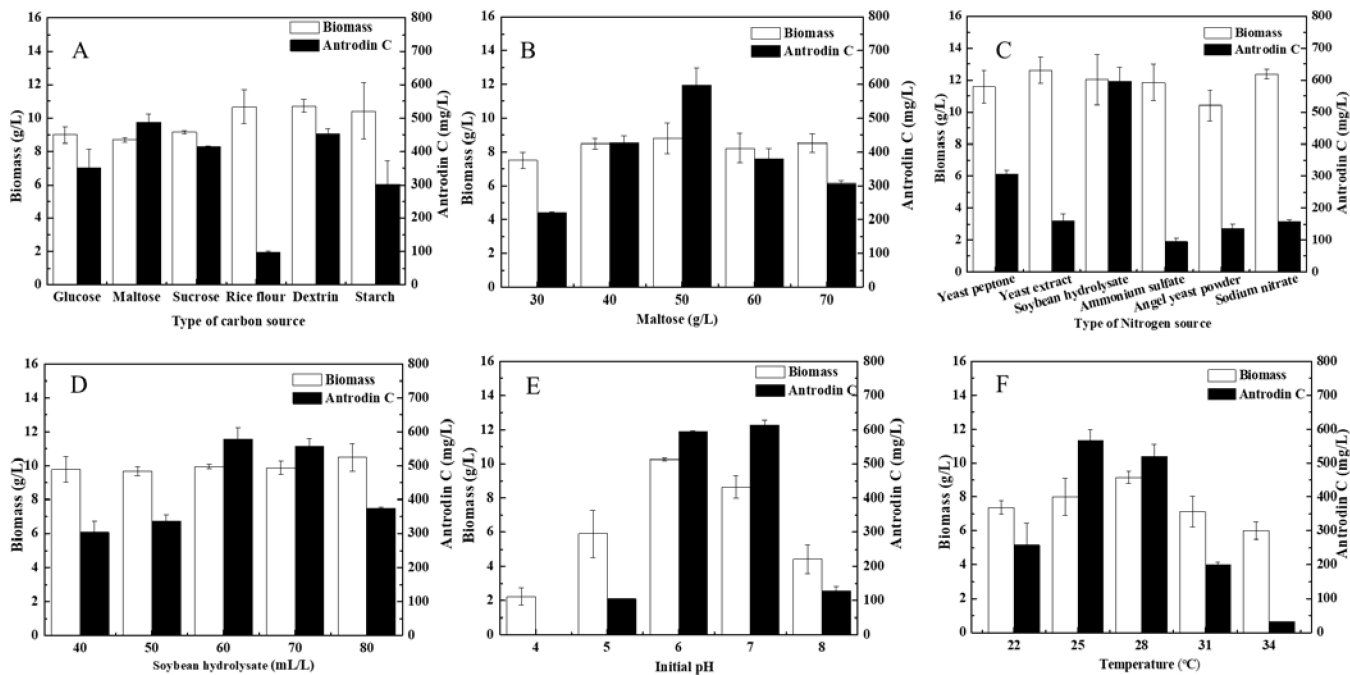


**Fig 4. Optimization of media constituents and fermentation temperature during antrodin C fermentation.**

A, Type of carbon source (each at 40 g/L, respectively); B, maltose concentration; C, type of nitrogen source (each at 6 g/L, respectively); D, concentration of soybean hydrolysate; E, initial pH; F, fermentation temperature. Biomass concentrations and antrodin C yields are shown as the mean  $\pm$  SD calculated from three independent experiments.



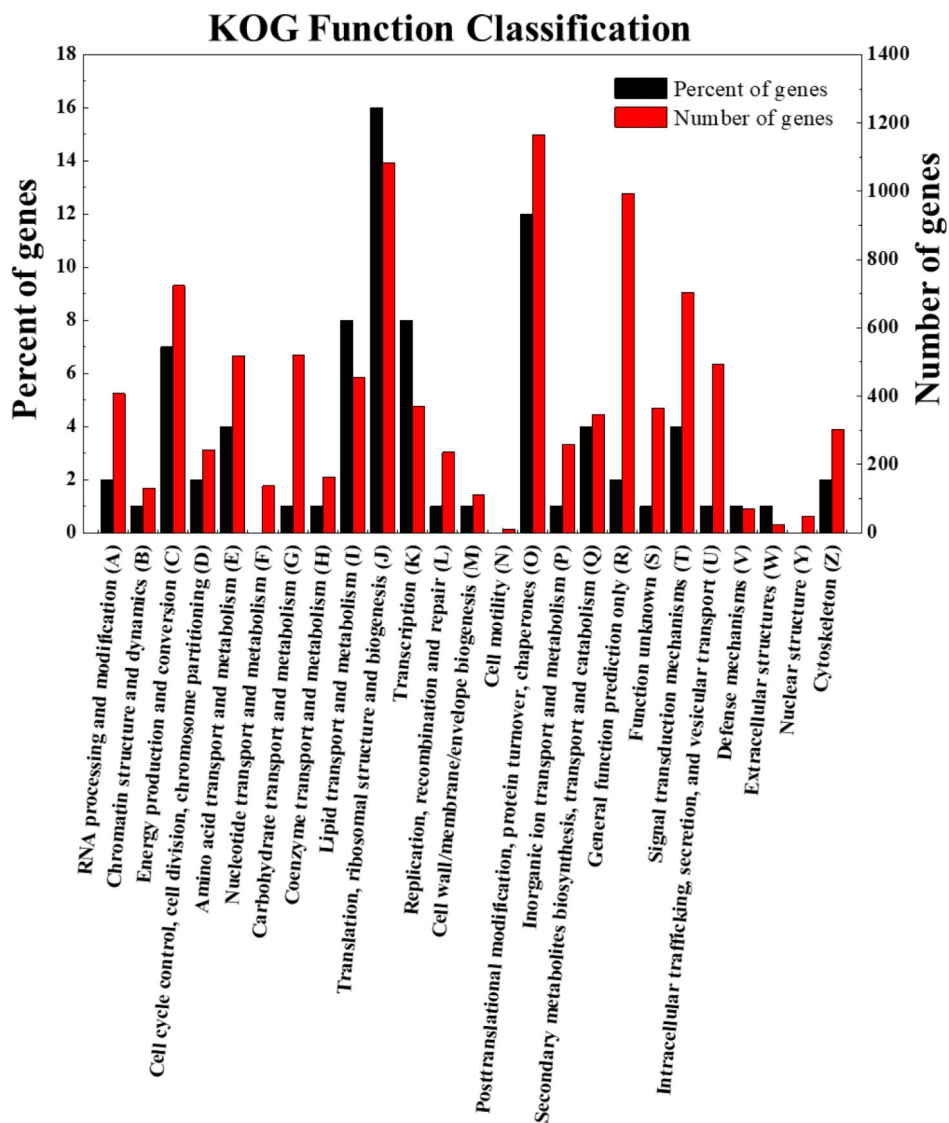


Fig. 5

**Fig 5. Functional annotation of differentially expressed genes upon H<sub>2</sub>O<sub>2</sub> supplementation during *A. cinnamomea* fermentation.**

DEGs were annotated with A, Gene Ontology; B, Kyoto Encyclopedia of Genes and Genomes; and C, Eukaryotic Orthologous Groups classifications.



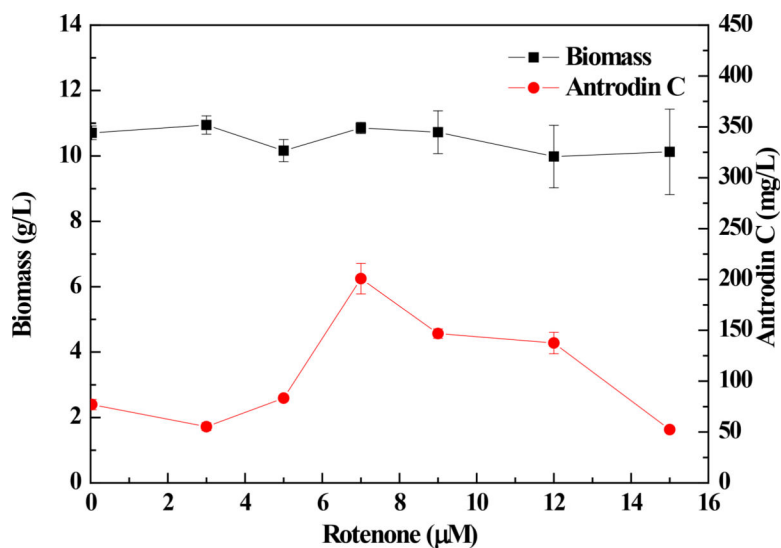


Fig. 6

**Fig 6. Effect of rotenone on the biomass accumulation and the production of antrodin C in submerged fermentation of *A. cinnamomea*.**

Biomass concentrations and antrodin C yields are shown as the mean  $\pm$  SD calculated from three independent experiments.

**Table 1.**

Effective concentrations of various antioxidants

Free radical <sup>1</sup>	Measure	Antrodin C	Vitamin C	BHA <sup>2</sup>	Vitamin E	Glutathione
ABTS•	TEAC <sup>3</sup>	0.2929 ± 0.0183	0.9834 ± 0.0636	3.5688 ± 0.1690	0.9864 ± 0.0453	1.3169 ± 0.0185
OH•	EC <sub>50</sub> <sup>5</sup>	0.7925 ± 0.0189	0.3729 ± 0.0158	ND <sup>4</sup>	0.7973 ± 0.0013	0.7002 ± 0.0211
DPPH•	EC <sub>50</sub>	0.0015 ± 0.00004	0.0006 ± 0.00009	0.0034 ± 0.0001	0.0039 ± 0.0002	0.0002 ± 0.00003

<sup>1</sup>ABTS•, 2,2'-azinobis-3-ethylbenzothiazoline-6-sulfonate radical; OH•, hydroxyl radical; DPPH•, 2,2-diphenyl-1-picrylhydrazyl radical

<sup>2</sup>BHA, Butylated hydroxyanisole

<sup>3</sup>TEAC, Trolox-equivalent antioxidant capacity [mM]

<sup>4</sup>ND, Not determined.

<sup>5</sup>EC<sub>50</sub>, 50% effective concentration [mg/mL]

**Table 2**

Repression of genes involved in the electron transport chain

Gene ID	$\log_2 \text{FoldChange} $	Function
TRINITY_DN317_c0_g1	-4.38	ATP synthase subunit 9
TRINITY_DN10718_c0_g1	-3.38	Cytochrome c and quinol oxidase polypeptide I
TRINITY_DN10718_c0_g3	-4.43	Cytochrome b
TRINITY_DN22851_c0_g1	-4.92	NADH dehydrogenase subunit 5
TRINITY_DN10352_c0_g1	-12.96	Oxidoreductase activity, acting on NAD(P)H, quinone or similar compound as acceptor
TRINITY_DN9064_c0_g1	-4.45	Mitochondrial ADP/ATP carrier proteins

Author Manuscript

Author Manuscript

Author Manuscript

Author Manuscript